

# The use of standardized infinity reference in EEG coherency studies

L. Marzetti,<sup>a,\*</sup> G. Nolte,<sup>c</sup> M.G. Perrucci,<sup>a</sup> G.L. Romani,<sup>a,b</sup> and C. Del Gratta<sup>a,b</sup>

<sup>a</sup>Department of Clinical Sciences and Biomedicine, Gabriele D'Annunzio University, Italy

<sup>b</sup>Institute for Advanced Biomedical Technologies, Gabriele D'Annunzio University Foundation, Italy

<sup>c</sup>Fraunhofer First, Berlin, Germany

Received 17 July 2006; revised 9 February 2007; accepted 10 February 2007  
Available online 3 March 2007

**The study of large scale interactions in the brain from EEG signals is a promising method for the identification of functional networks. However, the validity of a large scale parameter is limited by two factors: the use of a non-neutral reference and the artifactual self-interactions between the measured EEG signals introduced by volume conduction. In this paper, we propose an approach to study large scale EEG coherency in which these factors are eliminated. Artifactual self-interaction by volume conduction is eliminated by using the imaginary part of the complex coherency as a measure of interaction and the Reference Electrode Standardization Technique (REST) is used for the approximate standardization of the reference of scalp EEG recordings to a point at infinity that, being far from all possible neural sources, acts like a neutral virtual reference.**

The application of our approach to simulated and real EEG data shows that the detection of interaction, as opposed to artifacts due to reference and volume conduction, is a goal that can be achieved from the study of a large scale parameter.

© 2007 Elsevier Inc. All rights reserved.

---

## Introduction

The study of the functional relationships between brain areas has been one of the key issues ever since electroencephalography (EEG) has become a standard technique for brain study. To identify functional networks in the brain, different indices of the dynamic interaction between cortical areas have been used to quantify the relationship between regions that have a direct connection between each other or a common input from other cortical regions, or both (Nunez, 2000). Among these indices, scalp recorded EEG coherency is a large scale measure based on the frequency domain properties of the EEG recordings (Nunez et al., 1997), the cross-spectral density function, and the auto spectral density function, also called 'power spectrum', that has gained importance with the development of digital computation and new computational algo-

ritms (Cantero et al., 2000). Scalp recorded EEG coherency is, in general, a complex quantity, the modulus and phase of which have been used to establish the pattern of cortico-cortical interactions related to different functional states of the brain. In the decades passed since the first uses of coherence analysis in EEG, this technique proved to be a useful tool, both in healthy persons and in those with various diseases in which alterations in cerebral function are observed (Cantero et al., 2000). However, the validity of this parameter may be limited by discrepancies between the scalp coherency, intended as a projection of neural source interactions onto the scalp, and the actual coherency between underlying neural sources. Possible causes of these discrepancies are the volume conduction effect and the reference electrode effect. The former is the smearing distortion effect on the EEG generated by spatial low pass properties of the mapping of source to sensor activities. Therefore, when studying the interaction between signals (large scale interaction), the spread of the source activity to the channels enhances the degree of coherence between channels independently of the actual source interaction. The latter is the bias introduced in the estimated coherency maps by the non-neutrality of the signal at the reference electrode, which turns, usually, into overestimated coherency although erroneous underestimations at some site may also occur (Nunez et al., 1997).

In this work we propose an approach to study large scale EEG coherency that minimizes both the effect of the artifact introduced by volume conduction and that of the reference activity. The spatial filtering by volume conduction introduces an artifactual self-interaction in the classical coherency measure (i.e. the magnitude of the complex coherency) that does not show in the imaginary part of complex coherency. It can be shown, in fact, that this parameter, being insensitive to phenomena that do not have a time lag relative to each other, is insensitive to the artifactual 'self-interaction' caused by volume conduction, which is, under the quasi-static approximation, an instantaneous phenomenon (Nolte et al., 2004). Concerning the goal of reducing the effect of the reference choice, we propose the application of the Reference Electrode Standardization Technique (REST) (Yao, 2001; Yao et al., 2005) to obtain EEG signals referenced to a neutral reference. In fact, when measuring EEG signals, the reference location should be chosen so that this reference does not induce artificial structures e.g. due to

---

\* Corresponding author. Institute for Advanced Biomedical Technologies, Gabriele D'Annunzio University, Via dei Vestini, 33, 66013 Chieti (CH), Italy. Fax: +39 0871 3556930.

E-mail address: lmarzetti@unich.it (L. Marzetti).

Available online on ScienceDirect (www.sciencedirect.com).

sources close to the reference or due to the fact that the reference breaks rotational symmetry. The infinity reference has these properties and can be considered as neutral in this sense. In this way, the potential difference actually measured by the channels would show the same time course and therefore the same spectral properties of the ideal monopolar signals. Unfortunately, such a neutral reference is not attainable. Hence, the channel output results from a combination of activity at both the recording site and the reference site. It is worthwhile to underline that ‘classical’ common references introduce the undesired bias described above because the signal used as a reference may contain a significant part of information and is far from being neutral (Offner, 1950; Nunez et al., 1997; Dien, 1998). This may turn into erroneous physiological interpretation of coherence estimates. Other popular references are the digitally linked ears or the digitally linked mastoids, in which the signal obtained as a linear combination of the potentials measured at the ear or mastoid sites is used as a virtual reference electrode (Nunez et al., 1997). However, the effect of this kind of reference is to correlate data from the recording electrodes near the two mastoids (Srinivasan et al., 1998) and the neutrality of this kind of reference may vary according to the experimental and environmental conditions.

To reference data to a reliable neutral reference, we applied the REST method described by Yao (Yao, 2001; Yao et al., 2005) that proved to be efficient in recovering the waveform and the spectral properties of the potential referenced at infinity. The basic idea is the observation that the minimum norm estimation of the neural source activity from the scalp potential is not affected by the reference choice, provided that the reference is explicitly incorporated into the model (Geselowitz, 1998; Huizenga and Molenaar, 1996). An estimation of the infinity reference potential is obtained offline from any EEG data set, independently of the actual physical reference. Data transformed in this way (i.e. standardized data) already proved to be useful for frequency power mapping (Yao, 2001), in this work we extend the use of standardized data to coherency mapping. We show that the combined use of standardized data and of the imaginary part of complex coherency yields coherency maps that are free from artifacts due to reference and volume conduction and, therefore, their interpretation in terms of the underlying brain interactions can be more straightforward.

Furthermore, the proposed approach presents the advantages of a standardized referencing procedure: EEG signals acquired from different laboratories or stored with respect to various physical references in a database collected over time can be a posteriori uniformed, even if different environmental conditions or historical reasons required the use of different types of physical references in the acquisition procedure. Therefore, spectral and coherency studies can be performed on a reliable common basis and their results can be fairly compared.

## Materials and methods

The effectiveness of the REST method in recovering EEG recordings with a reference at infinity and the use of the recovered standardized signals for the calculation of coherency maps are investigated through the generation of simulated EEG potentials and through the application of the method to real EEG data. The dipole parameters and the time courses for each of the chosen configurations used in the generation of the simulated data are described in the following. No noise has been added to the simulated potentials except when explicitly noticed.

## Generation of simulated EEG potentials

Two simple configurations consisting of two symmetric dipoles of unit strength located at  $-6.4, 0.18, 4.9$  cm and  $6.4, 0.18, 4.9$  cm in the source space bounded by the innermost shell of the volume conductor model, the diameter of which is 15.9 cm, have been used. The dipoles are vertically oriented, along the  $z$ -axis, for the first source configuration shown in Fig. 1 (simulation 1) and horizontally oriented, along the  $y$ -axis, for the second (simulation 2). These two configurations have been chosen in order to evaluate the effect of dipole orientation.

For both of the simulations, the dynamics of the sources is represented by a Gaussian function

$$h(t_i) = \exp\left(-\left(2\pi f \frac{t_i - t_0}{\gamma}\right)^2\right) \cos(2\pi f(t_i - t_0) + \alpha) \quad (1)$$

with  $i=1, K, 256$ ,  $t_i=i \cdot dt$ ,  $dt=4$  ms,  $t_0=80 \cdot dt$ ,  $f=8$  Hz,  $\gamma=6$ ,  $\alpha=\pi/2$  for the first dipole and  $t_0=60 \cdot dt$ ,  $f=8$  Hz,  $\gamma=10$ ,  $\alpha=\pi$  for the second.

This function was chosen because it resembles an evoked potential. In principle, any temporal dynamics of the source propagated to the channels can be transformed using the REST method (Yao, 2001). The function parameters have been chosen to reproduce the condition of two coherent dipoles.

Given the dipole parameters and time courses, the EEG forward problem has been solved for the 3-shell spherical volume conductor model and an electrode montage given by 32 electrodes positioned in accordance with the International 10–20 electrode system.

The electric potentials were calculated using a spherical harmonics expansion in a standard way (Nunez and Srinivasan, 2006) omitting the constant with the effect that the average over the entire outermost surface is always zero. If such a potential is expanded to the external space by a harmonic function with the boundary conditions that the potential is continuous at the surface of the volume conductor and that the electric field vanishes at infinity and also imposing the constraint that the total charge inside an arbitrary sphere containing the head is zero, then also the potential vanishes at infinity. This potential will be indicated by  $V_{\text{inf}}$  in the following.

The potentials referred to the average, the cephalic and the digitally linked mastoids references, indicated by  $V_{\text{avg}}$ ,  $V_{\text{Fcz}}$  and  $V_{\text{dlm}}$  respectively, have been derived from the infinity reference potential according to the appropriate linear transformation. In particular, the digitally linked mastoids reference signal has been modeled by the average of the Tp9 and Tp10 channels that are located in the proximity of the mastoids.

The simulated potential has been transformed according to the REST method, and a reconstruction of the infinity reference potential has been derived.

In simulation 3, the effect of the source depth on the standardization performance is investigated. To this end, the left source of simulation 1 was kept fixed at the position  $[-6.4, 0.18, 4.9]$  cm and the right source depth ( $x$  coordinate) was varied in steps of 1 cm (Fig. 2).

The dynamics of the sources are modeled by Eq. (1) with the same parameter choice of simulation 1 and simulation 2. For each of the obtained source configurations, the surrogate  $V_{\text{avg}}$ ,  $V_{\text{Fcz}}$  and  $V_{\text{dlm}}$  data were derived as before, the standardization technique was applied and its performance as a function of source depth was evaluated.

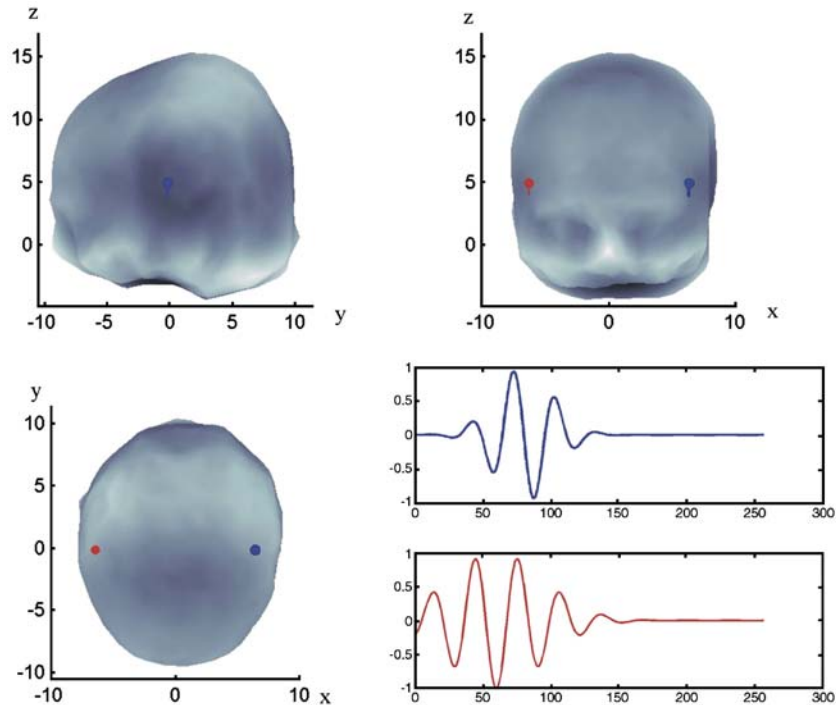


Fig. 1. Source parameters and time courses used in the case of two vertically oriented dipoles (simulation 1). The same configuration except for the horizontal orientation of the dipoles is used in simulation 2. These source parameters and time courses are used also in the case of simulation 4 in which noise is added to the simulated potential.

To investigate the effects of noise on the results of standardization, simulation 4 has been carried out in which Gaussian white noise has been added independently to all channels in the simulated data starting from a small noise level (8 dB signal-to-noise ratio) up to a large noise level (0.5 dB signal-to-noise ratio). Then, the infinity reference potential was reconstructed from the noisy data.

Finally, the effect of the presence of coherent and non-coherent sources as generators of the data has been analyzed (simulations 5 and 6) with a more complicated source configuration. The configuration consists of three sources, two of which are the same as those used for simulation 1 and the third is an occipital source located at  $[3.50 \ 5.19 \ 6.89]$  and oriented as  $[-1 \ 0 \ 1]$  (Fig. 3). The dynamics of the sources is simulated by Eq. (1) with  $i=1, K, 256$ ,  $t_i=i \cdot dt$ ,  $dt=4$  ms,  $t_0=80 \cdot dt$ ,  $f=8$  Hz,  $\gamma=6$ ,  $\alpha=\pi/2$  for the first dipole, with  $t_0=60 \cdot dt$ ,  $f=8$  Hz,  $\gamma=10$ ,  $\alpha=\pi$  for the second dipole and with  $t_0=100 \cdot dt$ ,  $f=8$  Hz,  $\gamma=15$ ,  $\alpha=0$  for the third, in case the three sources are all coherent (simulation 5), or with  $t_0=80 \cdot dt$ ,  $f=30$  Hz,  $\gamma=15$ ,  $\alpha=0$  for the third dipole, representing a case in which the third source is not coherent with the other two (simulation 6).

#### Application to real EEG data

As an example of the applicability of the proposed method to real EEG data, human spontaneous activity in one subject has been recorded using the BrainAmp MR (Brainproducts, Munich, Germany) EEG amplifier and the BrainCap electrode cap (Falk Minow Services, Herrsching-Breitbrunn, Germany) with sintered Ag/AgCl ring electrodes providing 29 EEG channels, 2 ECG channels and 1 EOG channel. They were positioned according to

the 10–20 system. The reference electrode was predefined in the cap and positioned between Fz and Cz. Raw EEG was sampled at 5 kHz using the Brain Vision Recorder software (Brainproducts). A four-minute epoch was recorded while the subject kept his eyes closed.

The processed EEG was visually inspected for eye movements, gross motion, and other artifacts. After down sampling to 1 kHz the EEG data set was used for the derivation of the standardized potential and the coherency mapping. The same potential referred to other references, such as average and digitally linked mastoids, has been also derived from the measured data for a comparison with the standardized potential. Coherency analysis based on the traditional coherency measure and on the proposed one (i.e. imaginary coherency) in the alpha band has been performed.

#### Reference Electrode Standardization Technique

The REST method is extensively described in Yao (2001) and Yao et al. (2005) and the interested reader is addressed to these references. However, for the sake of clarity, we briefly summarize the basics of the method in the following.

The premise of the method is the general relationship between the scalp recordings with respect to a body reference or with respect to the infinity reference, and the neural source. To describe this relationship we consider the general setting of an arbitrary source represented by an array of current dipoles fixed in location and direction. Specifically, we will consider as a source model a set of  $m$  current dipoles, the locations and directions of which are fixed in time whereas the strengths vary in time and are defined by the vector  $\mathcal{S}(t)$  with  $m$  components, where  $m$  is the number of dipoles in the source model and  $t$  is the time. The relationship between the

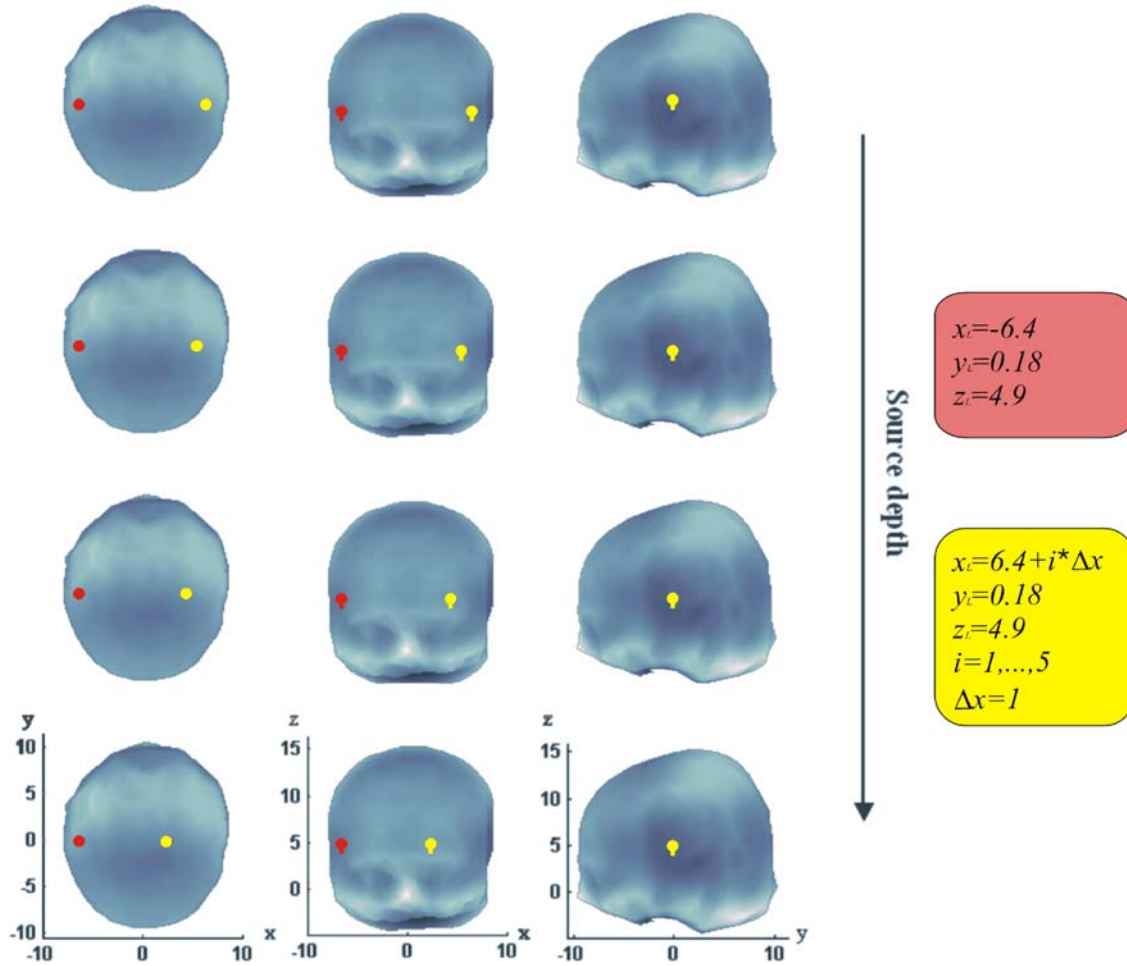


Fig. 2. Some of the source configurations used for simulation 3. The coordinates of the fixed dipole (right hemisphere) are indicated with  $(x_R, y_R, z_R)$ , the coordinates of the dipole in the right hemisphere are indicated with  $(x_L, y_L, z_L)$ .

dipole strengths  $\mathcal{S}(t)$  and the potential generated by the source is linear (Sarvas, 1987), and, for an infinity reference presuming zero scalp noise, can be expressed by the equation:

$$\mathbf{V}(t) = \mathbf{G}\mathcal{S}(t) \quad (2)$$

$\mathbf{V}(t)$  is a vector with  $n$  components where  $n$  is the number of EEG channels and  $\mathbf{G}$  is a transfer matrix of size  $n \times m$  ( $n < m$  in our model), called the EEG lead-field matrix.  $\mathbf{G}$  depends on the chosen head model, the location and the direction of the dipoles comprising the source model and the electrode montage.

If the reference is not set at infinity but at a different physical point  $R$ , the forward EEG calculation turns into:

$$\mathbf{V}_R(t) = \mathbf{G}_R \mathcal{S}(t) \quad (3)$$

where  $\mathbf{V}_R(t)$  is the vector of potentials referenced to the point  $R$  and  $\mathbf{G}_R$  is the EEG lead-field matrix for the  $R$  reference. The so-called linear inverse problem consists in the estimation of the strengths of the dipoles from the measured potential, i.e. the estimation of the  $\mathcal{S}(t)$  vector. In the following, we will indicate with  $\hat{\mathcal{S}}(t)$  the estimate of  $\mathcal{S}(t)$ . The inverse problem solution is not affected by the reference choice (Geselowitz, 1998; Pascual-Marqui and Lehmann, 1993; Yao, 2001), therefore, the same source estimate  $\hat{\mathcal{S}}(t)$  can be derived

either from Eq. (2) or from Eq. (3) solving the EEG inverse problem with a minimum norm solution based on the Moore–Penrose generalized inverse (denoted by the symbol  $\dagger$  in the following), as:

$$\hat{\mathcal{S}}(t) = \mathbf{G}^\dagger \mathbf{V}(t) \quad (4a)$$

$$\hat{\mathcal{S}}(t) = \mathbf{G}_R^\dagger \mathbf{V}_R(t) \quad (4b)$$

To the purpose of obtaining an estimate of the infinity reference potential, it is convenient to derive the source estimate from Eq. (3) as in Eq. (4b). Then, the reconstructed infinity reference potential, indicated by  $\mathbf{V}_{std}$  in the following, is obtained from Eq. (2) as:

$$\mathbf{V}_{std}(t) = \mathbf{G}\hat{\mathcal{S}}(t) = \mathbf{G}(\mathbf{G}_R^\dagger \mathbf{V}_R(t)) = \mathbf{U}_R \mathbf{V}_R(t) \quad (5)$$

where

$$\mathbf{U}_R = \mathbf{G}\mathbf{G}_R^\dagger \quad (6)$$

Given two arbitrary potentials,  $\mathbf{V}_{R1}$  and  $\mathbf{V}_{R2}$ , the sources for these potentials can be derived either from  $\mathbf{V}_{R1}$  or from  $\mathbf{V}_{R2}$  using Eq. (4b). The two estimates of the sources are exactly identical thanks to the independence of the minimum norm inverse problem

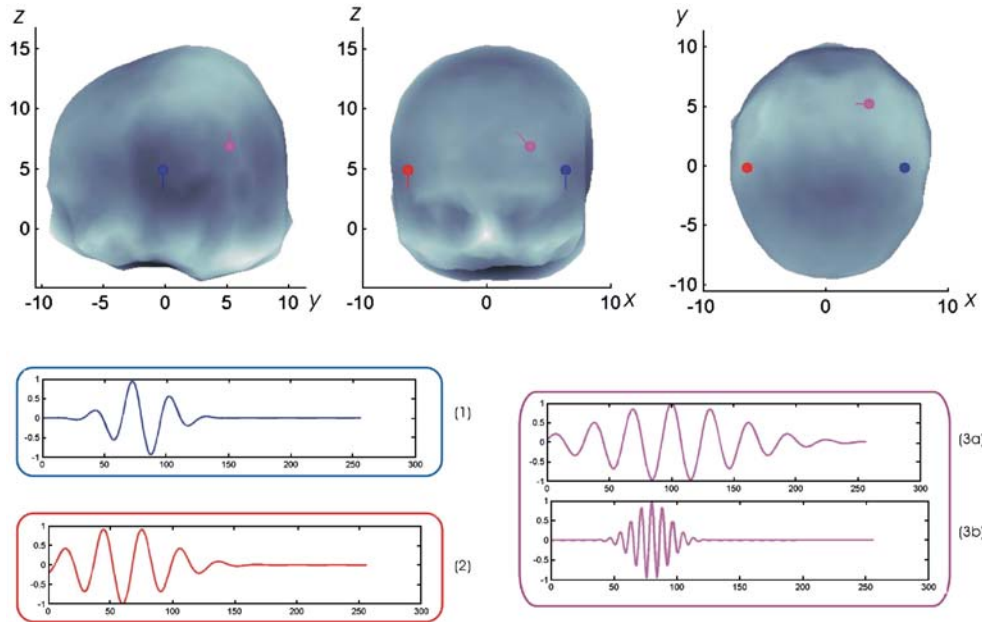


Fig. 3. Source parameters and time courses used in the case of simulation 5 and 6. The time course of the third source is given by plot 3a in case all of the three dipoles are coherent and by 3b in case only two out of three sources are coherent.

solution on the adopted reference, as observed above. For this reason, the reconstructed infinity reference potential  $V_{\text{std}}$  is the same regardless of the original reference of the potential.

Eq. (5) is the fundamental equation the REST method is based on. Eq. (5) indeed defines a re-referencing because  $V_{\text{std}}$  and  $V_R$  only differ by a constant since one can recover  $V_R$  from  $V_{\text{std}}$  simply by re-referencing to the original reference. A reconstruction of the potential referenced at infinity can be obtained simply by applying Eq. (5) since the matrices  $\mathbf{G}$  and  $\mathbf{G}_R$  are known and the matrix  $\mathbf{U}_R$  can be obtained from Eq. (6) once the Moore–Penrose generalized inverse of the matrix  $\mathbf{G}_R$  has been computed. This means that the knowledge of the source generating the measured potential distribution is not needed, in other words there is no need to solve the EEG inverse problem explicitly because the source is not directly involved in Eq. (5). Since we are not interested in the source themselves rather in the standardization re-referencing, no further regularization of the pseudoinverse has been used. In principle, any source distribution which is sufficiently general to parameterize arbitrary measurements and which generates smooth potentials can be used to derive the lead-field matrices  $\mathbf{G}$  and  $\mathbf{G}_R$ . The generation of the REST solution is then a model-based extrapolation for which the model is only used to estimate a spatial constant, which neutralizes the reference. We may therefore assume an equivalent source distribution (ESD) (Yao, 2003) and solve the EEG forward problem, obtaining  $\mathbf{G}$  and  $\mathbf{G}_R$ . Given the ESD, the lead-field matrices are determined by the head model and the electrode montage only (Yao, 2001).

In this work, as an ESD we use a dipole layer on a closed surface formed by a spherical cap, with radius defined on the basis of the head geometry, and a transverse plane. We used a discrete approximation of this closed surface consisting of 2700 dipoles perpendicular to the surface (Fig. 4). A realistic volume conductor, obtained from the MR images of the subject, can be used as a constraint for the definition of the dipole layer.

The EEG forward problem for the dipole layer is solved using a head representation based on a three-concentric-sphere model with normalized radii and conductivities 1.0 (brain and scalp) and 0.0125=1/80 (skull). The choice of a three-concentric-sphere model has been performed on the basis of the comparison of this volume conductor with the other two proposed by Yao (2001) and Zhai and Yao (2004): a simplified one-shell spherical model and a three-shell realistically shaped head model, respectively. When compared to the one-shell spherical model, the use of the three-shell spherical model results in a smaller relative difference between the standardized potential and the infinity reference potential than the one obtained using a single-shell model, although the standardization is still beneficial even using the oversimplified model. When compared to the three-shell realistically shaped head model, the use of the three-shell spherical model results into reduced sensitivity to the noise level in the data and into a relative error value that is comparable to the one obtained for the realistic model. For these reasons, we believe that the three-shell spherical model might represent a trade-off between the robustness of the method to noise and an accurate standardization.

The electrode montage is given by 32 electrodes positioned in accordance with the International 10–20 electrode system. Once the ESD model, the volume conductor model and the sensor configuration have been defined, the lead-field matrices for infinity reference, indicated as  $\mathbf{G}$ , and for the same physical reference to which the EEG data, either simulated or real, are referred (i.e. cephalic reference, average reference and digitally linked mastoids reference), generically indicated as  $\mathbf{G}_R$ , are calculated and the  $\mathbf{U}_R$  transformation is derived as in (6).

The simulated potentials referred to the cephalic, the average and the digitally linked mastoids references as well as the human spontaneous activity data have been transformed according to Eq. (5) and a reconstruction of the infinity reference potential has been obtained.

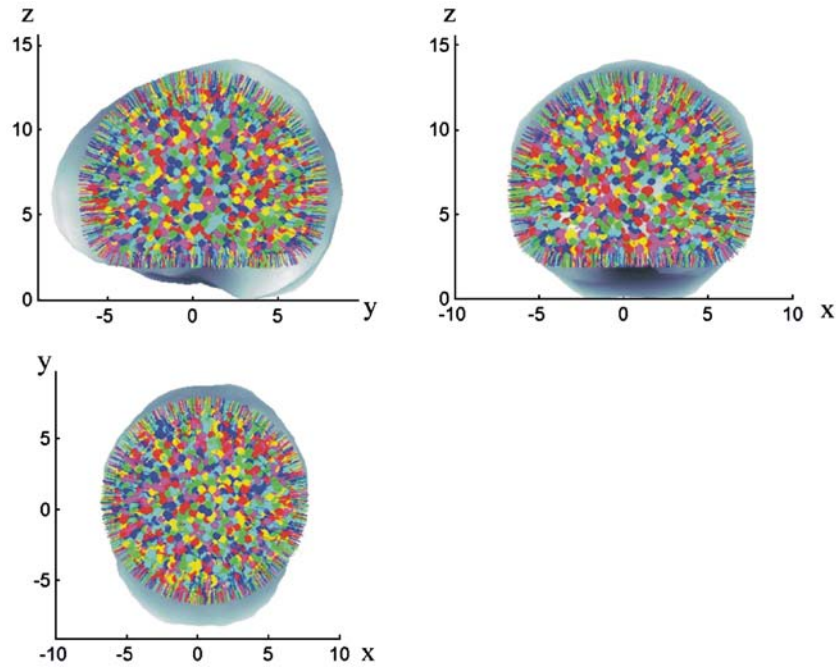


Fig. 4. Discrete dipole layer comprised of 2700 dipoles superimposed onto the inner skull obtained from MRI.

*Relative error for the potential*

In the case of simulated data, for which the theoretical infinity reference potential can be computed, the reconstructed potentials have been compared to this theoretical potential to assess the effectiveness of the standardization technique. The degree of similarity between the reconstructed potentials and the theoretical infinity reference potential has been assessed by calculating the

relative error (RE) for the EEG potentials according to the formula:

$$RE_{pot} = \frac{\|V_{inf} - V^*\|_F}{\|V_{inf}\|_F} \tag{7}$$

where  $V_{inf}$  is the theoretical spatio-temporal recording with reference at infinity and  $V^*$  is one of the recordings  $V_{Fcz}$ ,  $V_{avg}$

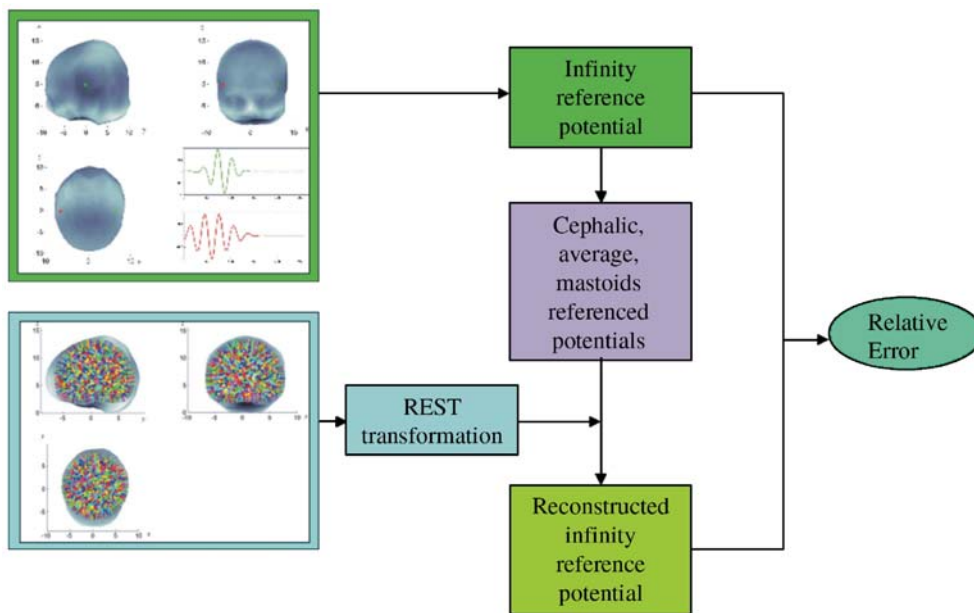


Fig. 5. Simulation scheme: the infinity reference potential is calculated from the source configuration, data are referenced to the chosen reference and the REST transformation, obtained through the solution of the forward problem for the dipole layer, is applied to the data yielding a reconstruction of the infinity reference potential. The correspondence between the theoretical infinity reference potential and the reconstructed one is evaluated in terms of the relative error.

and  $V_{\text{dlm}}$  as well as  $V_{\text{std}}$ . The matrix norm  $\|\cdot\|_F$  is the Frobenius norm, which for a generic matrix  $\mathbf{A}$  of size  $N \times T$  is defined as:

$$\|\mathbf{A}\|_F = \left( \sum_{i=1}^N \sum_{j=1}^M a_{ij}^2 \right)^{1/2} \quad (8)$$

The sum in Eq. (8) is a sum over time points and over channels, therefore the relative error in Eq. (7), taking into account both space and time domains, is a global indicator of the similarity between EEG signals.

The whole simulation procedure is schematically described in Fig. 5.

### Coherency

The coherency between two EEG channels is a measure of their linear relationship at a specific frequency  $f_0$ . It is expressed as:

$$C_{ij}(f_0) \equiv \frac{Cs_{ij}(f_0)}{(S_{ii}(f_0)S_{jj}(f_0))^{1/2}} \quad (9)$$

where

$$Cs_{ij}(f) \equiv \langle X_i(f)X_j^*(f) \rangle \quad (10)$$

is the cross-spectrum of the time series  $x_i(t)$  and  $x_j(t)$  of channel  $i$  and  $j$ .  $X_i(f)$  and  $X_j(f)$  in Eq. (10) are the Fourier transforms of the time series  $x_i(t)$  and  $x_j(t)$  obtained using the Fast Fourier Transform (FFT) algorithm.

The symbols  $*$  and  $\langle \cdot \rangle$  in Eq. (10) mean complex conjugation and expectation value, respectively. In practice, the expectation value can only be estimated as an average over a sufficiently large number of epochs because coherency depends on the unknown probability density function of the associated stochastic process represented by the EEG time series.

Coherency between EEG channels at a given frequency  $f_0$  is a square matrix of size  $n \times n$ . Its diagonal elements are equal to one, representing the correlation of each channel with itself, whereas all the other terms of the matrix are complex numbers. The full complex information is distinguished from its magnitude, given by:

$$\text{Coh}_{ij}(f_0) = |C_{ij}(f_0)| \quad (11)$$

which is the most popular coherency measure. As any complex number, each value in the coherency matrix can be expressed using two possible representations: Cartesian or polar. The latter is the modulus and phase representation whereas the former is the representation in terms of real and imaginary part. In this work, we will base the coherency study on the Cartesian representation of coherency as expressed by:

$$\text{Re}C_{ij}(f_0) + i\text{Im}C_{ij}(f_0) \quad (12)$$

In particular, the imaginary part in Eq. (12) represents that part of complex coherency which necessarily reflects brain interactions. To prove this, let us assume that the signals in channel  $i$  and  $j$  arise from a linear superposition of  $K$  independent sources  $s_k(f_0)$ :

$$X_i(f_0) = \sum_{k=1}^K a_{ik}s_k(f_0) \quad (13)$$

and similarly for  $X_j(f_0)$ . We further assume that mapping of sources to sensors is instantaneous, implying that the phases are not distorted resulting in real coefficients  $a_{ik}$ .

We then have for the cross-spectrum

$$\begin{aligned} Cs_{ij}(f_0) &\equiv \langle X_i(f_0)X_j^*(f_0) \rangle = \sum_k a_{ik}a_{jk} \langle s_k(f_0)s_k^*(f_0) \rangle \\ &= \sum_k a_{ij}a_{jk} \langle |s_k(f_0)|^2 \rangle \end{aligned} \quad (14)$$

which is real. Since the normalization by the channel spectra is also real, it follows immediately that coherency is also real. The assumption that the mapping of the sources to the sensors is instantaneous, i.e. signal conduction through the head is a process that does not introduce any time lag in the signal, is a direct consequence of the quasi-static approximation of the forward problem (Nolte et al., 2004). As a consequence of the fact that the complex coherency matrix for non-interacting sources is merely real we can derive that a non-vanishing imaginary part can only be due to interacting sources. Moreover, the instantaneous mapping of source activity into sensor signals makes the imaginary part of coherency insensitive to the artifactual ‘self-interaction’ caused by volume conduction.

This property of the imaginary part of coherency of being only sensitive to processes time-lagged to each other implies that perfectly synchronous sources do not contribute to the imaginary part of coherency but only to its real part and therefore cannot be detected using the imaginary part of coherency alone.

The channel spectra and cross-spectra have been estimated for the simulated spatio-temporal EEG recordings  $V_{\text{Fcz}}$ ,  $V_{\text{avg}}$  and  $V_{\text{dlm}}$  as well as for the corresponding standardized data  $V_{\text{std}}$  obtained from the above described configurations and for the real EEG data and the corresponding standardized version. Coherency between all channel pairs with 1 Hz frequency resolution has been then derived according to Eq. (9) and its imaginary part has been mapped.

In the following, we will indicate by  $C_{\text{avg}}$  the coherency matrix estimated from the potential referenced to the average reference  $V_{\text{avg}}$ . Similarly, we will use the notation  $C_{\text{Fcz}}$  to indicate the coherency matrix estimated from the potential referenced to the cephalic reference  $V_{\text{Fcz}}$  and  $C_{\text{dlm}}$  to indicate the coherency matrix estimated from the  $V_{\text{dlm}}$  potential. Furthermore, when dealing with simulated data, the notation  $C_{\text{inf}}$  is used for coherency matrix estimated from the infinity reference potential. The subscript std indicates that the quantity is obtained from the standardized potentials rather than from the original potentials  $V_{\text{avg}}$ ,  $V_{\text{Fcz}}$  and  $V_{\text{dlm}}$ .

### Relative error for coherency maps

Similarly to the case of the potentials, we assess the similarity between the maps of the imaginary part of the coherency for the simulated data by defining the relative error ( $\text{RE}_{\text{coh}}$ ) as:

$$\text{RE}_{\text{coh}} = \frac{\|\text{Im}(C_{\text{inf}}(f_0)) - \text{Im}(C^*(f_0))\|_F}{\|\text{Im}(C_{\text{inf}}(f_0))\|_F} \quad (15)$$

where  $C_{\text{inf}}(f_0)$  in Eq. (15) is the coherency matrix at frequency  $f_0$  calculated from  $V_{\text{inf}}$ , and  $C^*$  is one of the coherency matrices  $C_{\text{avg}}$ ,  $C_{\text{Fcz}}$ ,  $C_{\text{dlm}}$ ,  $C_{\text{std}}$ , respectively.

## Results and discussion

The discrepancies between the standardized and the theoretical infinity reference potential have been already investigated in Yao (2001) for various simulated data sets corresponding to different source configurations, electrode numbers and volume conductor

models (Zhai and Yao, 2004). Therefore, in the following, we will show the results for the spatio-temporal characteristic of the simulated data but we will mainly concentrate on the differences in spectral properties of the recovered and the theoretical infinity reference signals and their respective coherency maps at given frequencies of interest. The spectral and coherency properties of the standardized data, particularly in the alpha band, are the focus of interest also in the analysis of human spontaneous activity.

#### Results: potential

##### Simulated data

Fig. 6(a) shows the standardized potential  $V_{std}$  obtained applying the REST method to the simulated EEG recordings. The same simulated data referred to the average, cephalic and digitally linked mastoids are, respectively, shown in (b), (d) and (e). The resemblance between the standardized potential and the theoretical infinity reference potential, shown in (c), can be evaluated by a comparison of the time courses in Figs. 6(a) and (c) in reference to simulation 1. This figure shows, for a subset of channels, that the absolute and relative amplitude of the infinity reference potential for all the channels is restored by the standardized data.

Together with the temporal information shown in Fig. 6 we can look at the spatial pattern of the original, theoretical, and standardized signals. With reference to simulation 1, from the analysis of the channel maps at a given time instant (e.g. 50 ms) a high similarity between the standardized potentials and the theoretical infinity reference potential is observed, whereas in the map for the original  $V_{avg}$ ,  $V_{Fcz}$  and  $V_{dlm}$  the influence of the non-neutral reference turns into the presence of a strong positive pole (see Fig. 7).

The degree of similarity between the reconstructed potentials and the theoretical infinity reference potential and between the original potentials and the theoretical infinity reference potentials has been assessed by calculating the relative error according to Eq. (7). The results for both of the considered dipole orientations are shown in Table 1 and illustrate that, for vertically oriented dipoles, the standardized potential is a better approximation of the ideal condition than the original data. In particular, a factor of about 14 is gained in comparison with the digitally linked mastoids (dlm) reference, a factor of 40 in comparison to the average (avg) reference and a factor of 60 in comparison to the cephalic (Fcz) reference. In the case of the horizontal configuration (simulation 2), the standardization results are comparable to the avg reference and reach a twofold gain with respect to the Fcz reference and 8 times larger than the dlm reference. This result is in accordance with the findings of Yao (2001) for a 32-electrode cap: if the dipole orientations are such that RE between the average reference and the theoretical one is small, the standardization method is not able to get any further improvement and even a slight degradation of the RE can be introduced by the method. Furthermore, Table 1 shows that the choice of the optimal reference depends on the actual source positions and orientations.

In simulation 3, the performance of the standardization procedure for various source positions is evaluated for increasing depth of one of the sources according to the schema shown in Fig. 2. In Table 2, the values for the relative error of the simulated data for the digitally linked mastoids reference and the standardized reference (std) with respect to the theoretical data are listed. Among the three original references, only the dlm reference has been reported because this reference shows the best results before the standardization in

simulation 1. Our results show that, despite the degradation of the performances of the standardization with increasing source depth and the improvement of the performances of the digitally linked mastoids reference as the source moves away from the mastoid channel, the standardized reference always reaches an improvement larger than a factor of 2 and is, therefore, still beneficial.

#### Results: coherency maps

##### Simulated data

The simulated spatio-temporal EEG recordings  $V_{Fcz}$ ,  $V_{avg}$  and  $V_{dlm}$  as well as the standardized data  $V_{std}$  have been used for the derivation of the coherency maps (Eq. (9)). The imaginary part of the complex coherency maps at 8 Hz (main frequency of the simulated source signals) is shown in Fig. 8 for simulation 1 and in Fig. 9 for simulation 2. The single large circle in these figures is a 2-dimensional representation of the whole scalp and at each electrode position a small circle is placed representing the scalp and containing the imaginary part of the coherency of the respective electrode with all other electrodes, i.e. the  $i$ -th small circle contains the  $i$ -th row of the coherency matrix. The  $i$ -th channel (marked as a black dot in each small circle) is maximally coherent with the channels indicated either in blue or in red in the pictures. In order to avoid overlaps, the small circles have been slightly shifted using a dedicated iterative procedure.

From Figs. 8 and 9 we observe that the imaginary part of coherency for standardized data, (a), (b) and (c), shows a pattern similar to that of the infinity reference maps, (d). These observations are also supported by the results obtained for the relative errors reported in Table 3.

It can be seen, in fact, that whenever the standardization procedure is applied to the simulated data, a decrease of the relative error is obtained. In particular, regarding the most favorable condition of simulation 1, a factor of at least 25 is gained. In the second simulation we observe a small gain with respect to the avg reference, whereas a factor of 3 is gained in comparison to the dlm reference. In a real case the source can have any orientation, considering that in the worst case (horizontal orientation) the gain in the coherency is slightly larger than 1 we believe that the standardized potential should be preferred to other proposed references for the derivation of coherency maps. Moreover, the visual inspection of the maps for the imaginary part of coherency suggests that the use of the std reference eliminates the reference bias.

In the maps of the imaginary part of the coherency for the standardized  $V_{std}$  as well as for the infinity reference  $V_{inf}$  potentials, Fig. 8(c), a strong interaction between the channels in the left part of the EEG cap (i.e. electrodes close to the location of the left source) with those on the right part (i.e. electrodes close to the location of the right source) and, vice versa, between the channels in the right part of the EEG cap (i.e. electrodes close to the location of the right source) with those on the left part (i.e. electrodes close to the location of the left source), can be observed in the simplest case of simulation 1 at 8 Hz. It should be noted that while this pattern is correctly reconstructed by using the standardized reference (Fig. 8(a)), it is only very roughly reconstructed by using the average reference (Fig. 8(b)) or the linked mastoids reference (Fig. 8(e)), and strongly misreconstructed using the cephalic reference (Fig. 8(d)).

Although more complicated, in Fig. 9(c) (simulation 2) it can be observed that the 6 rightmost electrodes show the highest levels of coherency (either positive or negative) on the left hand side of the maps and vice versa the 6 leftmost electrodes show the highest

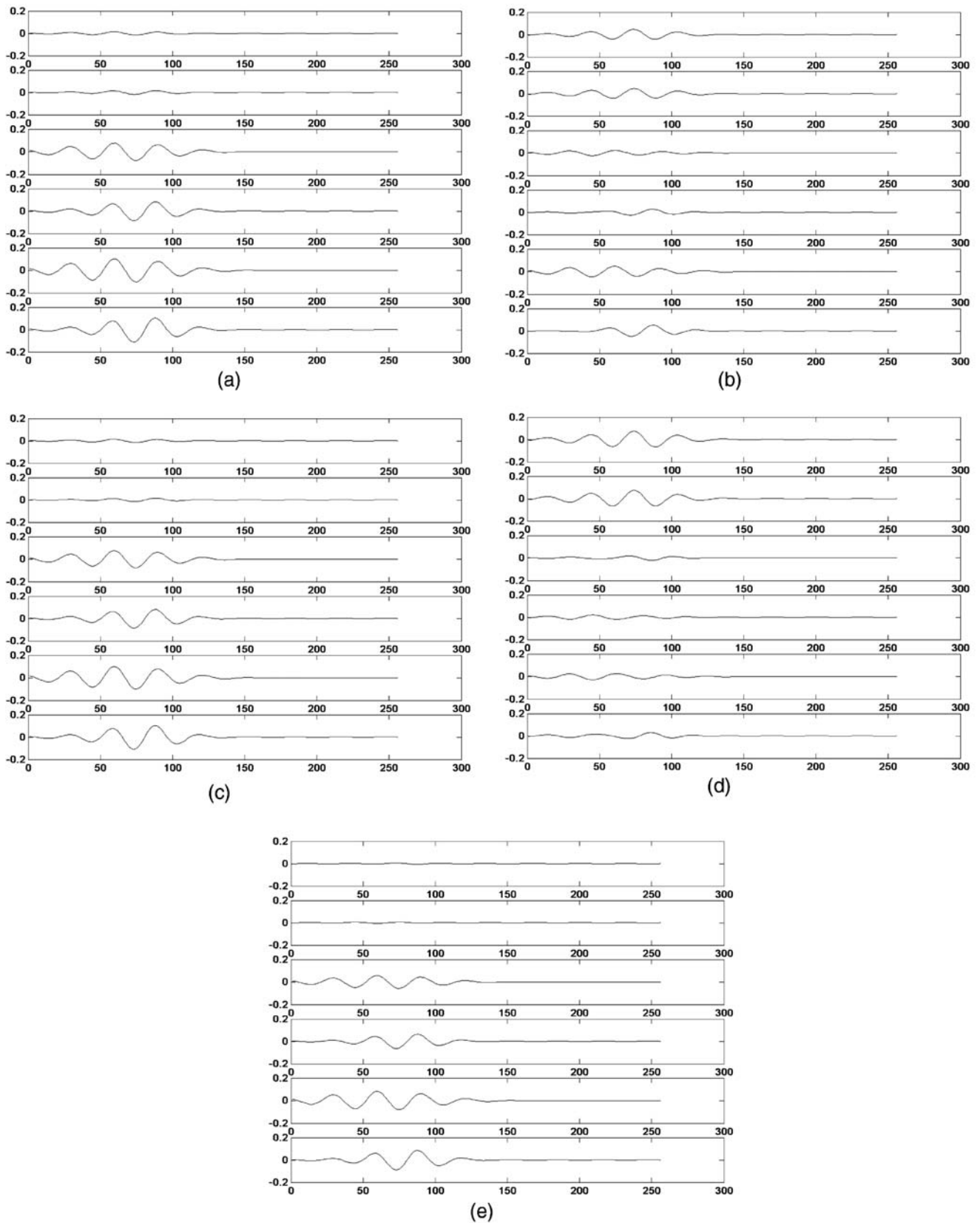


Fig. 6. Simulated potentials obtained in the case of two vertically oriented dipoles (simulation 1): the theoretical infinity reference potential is shown in the center (c), the REST reconstructed potential  $V_{std}$  is shown in the upper left (a), the potential referred to the average reference  $V_{avg}$ , to the cephalic reference  $V_{Fcz}$  and to the digitally linked mastoids reference  $V_{dlm}$  are shown in the lower left (b), in the upper right (d) and in the lower right (e), respectively.

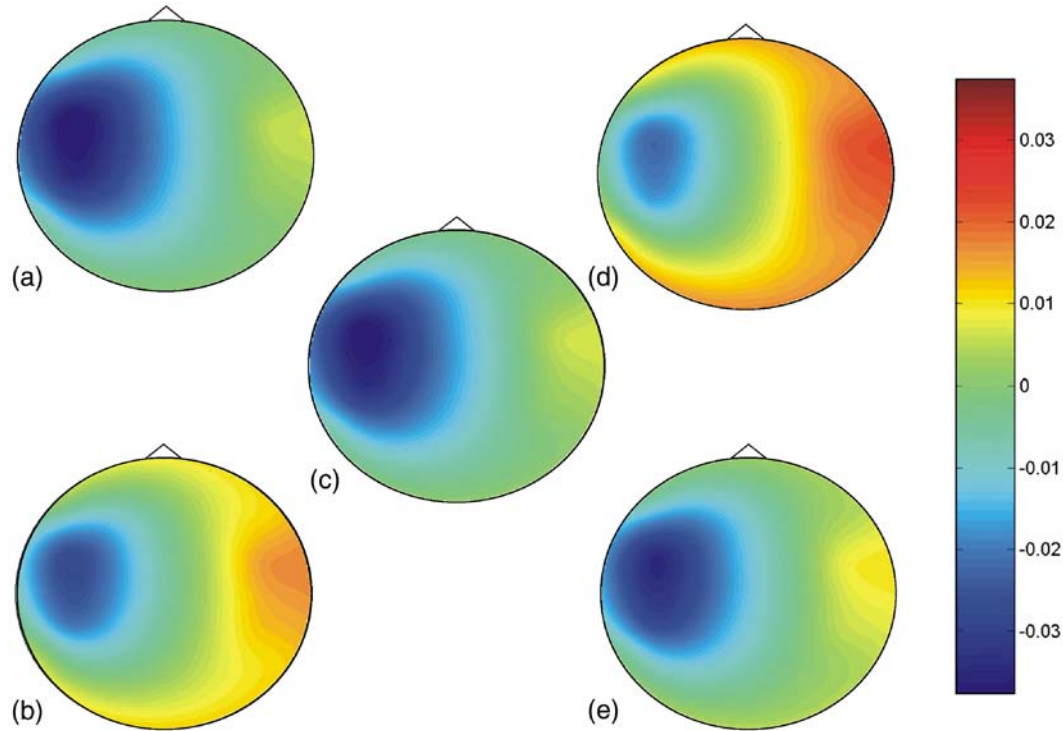


Fig. 7. Maps for the potentials obtained in the case of two vertically oriented dipoles (simulation 1). The map for the infinity reference potential  $V_{inf}$  is shown in the center (c) and can be compared to the REST transformed data  $V_{std}$  shown in the upper left (a), to the average reference potential  $V_{avg}$  shown in the lower left (b), to the cephalic reference potential  $V_{Fcz}$  shown in the upper right (d) and to the digitally linked mastoids reference potential shown in the lower right  $V_{dlm}$  (e).

levels of coherency (either positive or negative) on the right side of the maps. Here again it can be observed that the best reconstruction is obtained by using the standardized reference (Fig. 9(a)), although in this case the worst mis-reconstruction is given by the use of the linked mastoids reference (Fig. 9(e)). The reconstruction by means of the average reference is good in this case because the configuration with horizontal dipole sources generates a potential distribution that is symmetric with respect to the central left–right plane, so that the average potential over the scalp is close to zero. The reconstruction using the cephalic reference is acceptable because again due to the symmetry of the source configuration the potential at the cephalic electrode is low.

The interpretation of the coherency maps in such complicated cases can be guided by the cross-spectra pattern that can give hints on the underlying source configuration. Fig. 10 shows the maps for the imaginary part of the coherency estimated from  $V_{std}$  (a and d),  $V_{inf}$  (b and e), and  $V_{dlm}$  (c and f) for the most superficial and

deepest of the investigated configurations. It can be seen that, for the deepest source, although the coherency pattern for the standardized data (d) is significantly different from the corresponding infinity reference potential (e), an improvement is still obtained relative to the corresponding map for the original data (f). The relative error, reported in Table 4 for all the source configurations, shows, in fact, that the source depth influences the achieved similarity between the standardized and the theoretical coherency maps. Indeed, Yao (2001) reported that the REST method effectiveness in recovering the infinity reference potential depends, apart from the volume conductor model and the electrode number, also on the actual location of the dipole. In particular, the best results are obtained for sources located over the superficial regions of the cortex. Despite this degradation, still a factor of 5 is gained in the case of the deepest source location.

Simulation 4 aims at investigating the effectiveness of the standardization technique when noisy data are treated. The source

Table 1  
Relative errors between original and theoretical infinity reference data and between standardized data and theoretical infinity reference data for the vertical configuration of simulation 1 and for the horizontal configuration of simulation 2

Reference type	Simulation 1 ( $RE_{pot}$ )		Simulation 2 ( $RE_{pot}$ )	
	Original reference	std reference	Original reference	std reference
Average	0.85	0.02	0.12	0.15
Cephalic	1.25		0.32	
Dlm	0.29		1.36	

Table 2  
Relative errors between original and REST transformed and theoretical maps for the potential at various source depths for the dipole in the left hemisphere

Source position ( $x_L$ )	DLM reference ( $RE_{pot}$ )	STD reference ( $RE_{pot}$ )
5.4	0.27	0.01
4.4	0.25	0.04
3.4	0.24	0.06
2.4	0.23	0.08
1.4	0.23	0.09

The most superficial source is reported in the first row and the deepest in the last row.

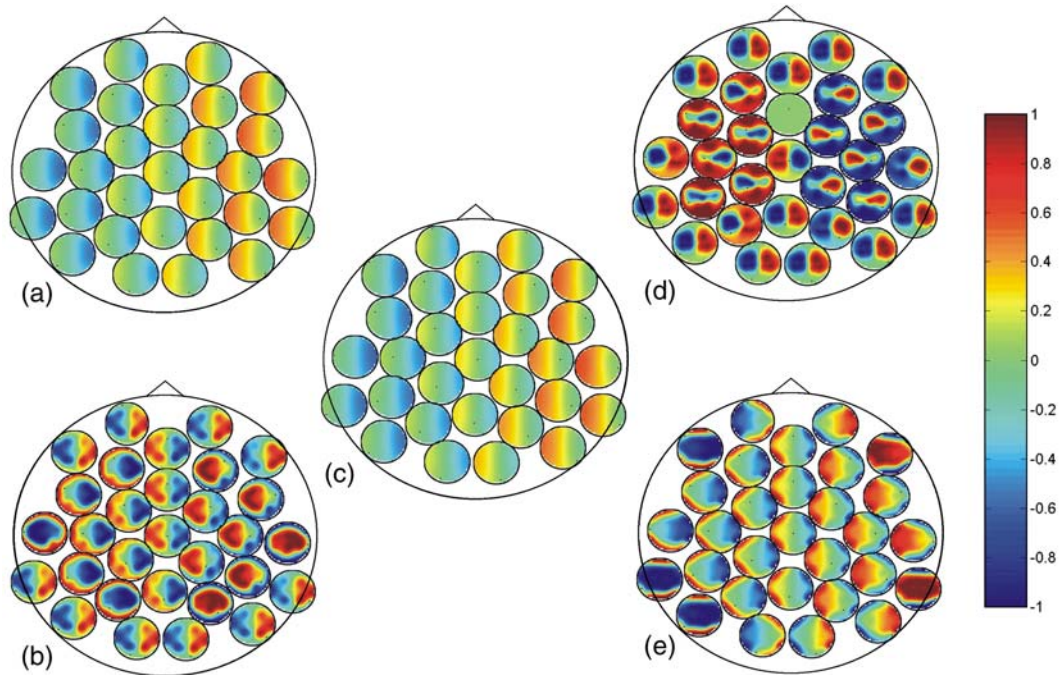


Fig. 8. Imaginary part of complex coherency (8 Hz) derived from simulation 1. The map for the coherency estimated from infinity reference potential data  $C_{inf}$  is shown in the center (c) and can be compared to the one estimated from standardized data  $C_{std}$ , shown in the upper left (a), to the one estimated from the average reference data  $C_{avg}$ , shown in the lower left (b), to the one estimated from cephalic reference data  $C_{Fcz}$ , shown in the upper right (d), and to the one estimated from digitally linked mastoids reference data  $C_{dlm}$ , shown in the lower right (e).

configuration used in this case is the same as in simulation 1. Noise of various levels has been added to the simulated data. The behavior of the standardization technique in the presence of noise has already been investigated by Yao in 2001. If simulated data

with infinity reference with superimposed noise of various levels are transformed with respect to cephalic, average digitally linked mastoids, and standardized references (simulation 4), and used to derive coherency maps, very similar patterns are obtained across

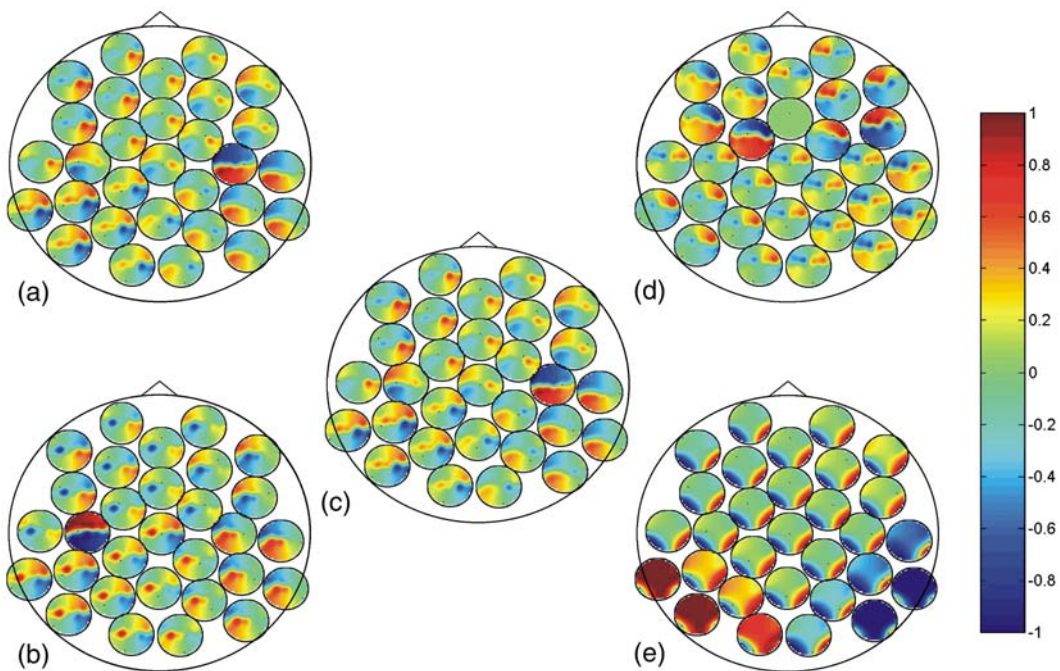


Fig. 9. Imaginary part of complex coherency (8 Hz) derived from simulation 2 (horizontally oriented dipoles). The maps are positioned as in Fig. 8:  $C_{std}$  (a),  $C_{avg}$  (b),  $C_{inf}$  (c),  $C_{Fcz}$  (d), and  $C_{dlm}$  (e), respectively.

Table 3  
Relative errors between original and infinity reference maps and between standardized data and infinity reference data maps for the imaginary part of the coherency

Reference type	Simulation 1 (RE <sub>pot</sub> )		Simulation 2 (RE <sub>pot</sub> )	
	Original reference	std reference	Original reference	std reference
Average	2.26	0.07	0.76	0.73
Cephalic	2.97		0.93	
Digitally linked mastoids	1.78		2.27	

signal-to-noise ratios. Although the noise corruption in the map becomes visible for a signal-to-noise ratio around 8 dB, it does not dramatically increase with decreasing the signal-to-noise ratio down to 0.5 dB (Fig. 11). In the case of cephalic, average and digitally linked mastoids noisy data, the pattern dissimilarity with respect to the theoretical infinity reference case is mainly due to the reference contribution to large scale coherency, and the effect of noise in the data plays a secondary role. In the case of the standardized potential, the reference effect has been eliminated and, of course, the noise is the main cause of the possible dissimilarity with the ideal case.

The simulations referred to as simulation 5 and simulation 6 take into account the complexity of the pattern for the imaginary part of the coherency arising from the presence of three dipoles. In

Table 4  
Relative errors between original and REST transformed and theoretical maps for the imaginary part of the coherency at various source depths for the dipole in the left hemisphere

Source position ( $x_L$ )	d1m reference (RE <sub>coh</sub> )	std reference (RE <sub>coh</sub> )
5.4	1.85	0.02
4.4	1.95	0.13
3.4	2.07	0.25
2.4	2.12	0.36
1.4	2.20	0.42

The most superficial source is reported in the first row and the deepest in the last row.

particular, these simulations aim at comparing the results for the imaginary part of the coherency, in the case when all sources are coherent and in the case when only two of them are coherent. The configuration used in these two cases is shown in Fig. 3. For the imaginary coherency, the case in which only two dipoles are coherent is equivalent to the case of only two dipoles (see Fig. 8 for a comparison). When the third dipole is coherent with the previous two, it affects the imaginary part of the coherency (Fig. 12). The similarity between the theoretical map (c) and the standardized one (a) is still high. The interpretation of the new maps is now more complicated, but in spite of this complexity, in Fig. 12(c) it is interesting to examine the temporo-occipital electrodes that are close to the source dipoles: if we consider the rightmost electrode

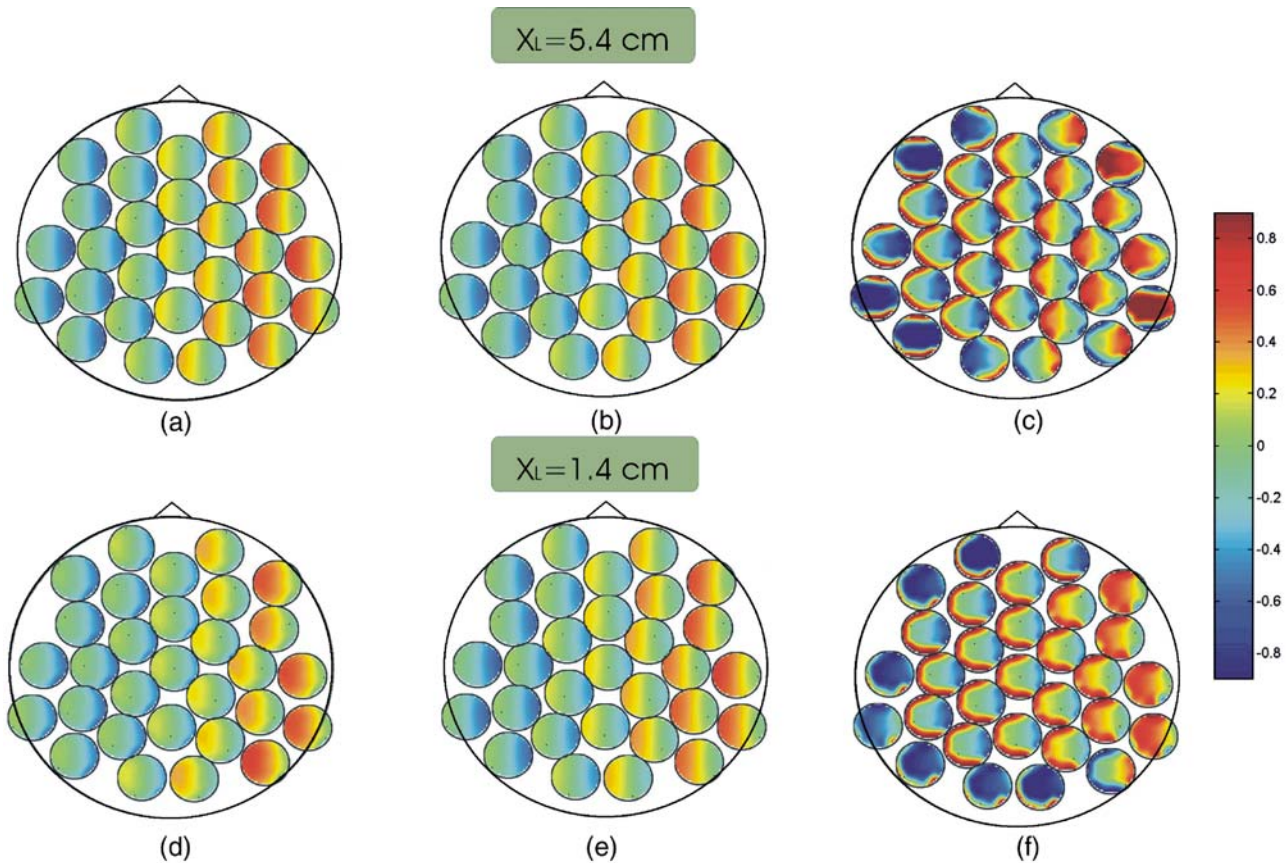


Fig. 10. Maps for the imaginary part of complex coherency (8 Hz) for one superficial configuration ( $x_L=5.4$  cm) for  $C_{std}$  (a),  $C_{inf}$  (b), and  $C_{d1m}$  (c) and for one deep configuration ( $x_L=1.4$  cm) for  $C_{std}$  (d),  $C_{inf}$  (e), and  $C_{d1m}$  (f) in the case of simulation 3.

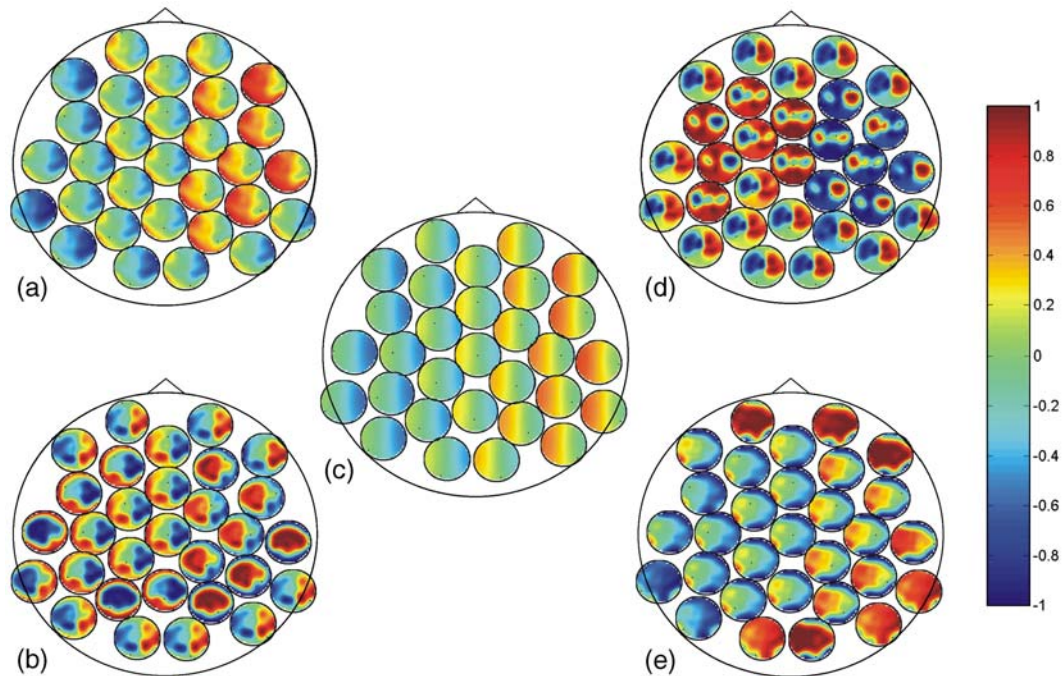


Fig. 11. Imaginary part of complex coherence (8 Hz) derived in the case of simulation 1 adding noise to the simulated data (SNR 0.5 dB). The map for the coherence estimated from infinity reference potential data without noise  $C_{inf}$  is shown in the center (c) and can be compared to the one estimated from standardized noisy data  $C_{std}$ , shown in the upper left (a), to the one estimated from the average reference noisy data  $C_{avg}$ , shown in the lower left (b), to the one estimated from cephalic reference noisy data  $C_{cep}$ , shown in the upper right (d), and to the one estimated from digitally linked mastoids reference noisy data  $C_{dlm}$ , shown in the lower right (e).

in the left–right central plane (electrode T4) we can see that it shows the highest levels of coherence with the left hand side electrodes (negative), maximally with T3 and with the temporo-occipital electrodes (positive) of the right side (O2 and T6). For comparison, on the right side of the head, the symmetric electrode T3 shows coherence (positive) only with the left side including the temporo-occipital electrodes (O2, T6 and T4). This asymmetry in the coherence pattern reflects the asymmetry of the source configuration. It should be noted here again that the coherence pattern in the simulated data (Fig. 12(a)) is accurately reconstructed by using the standard reference (Fig. 12(a)) but not by using the other references (Figs. 12(b, d, e)).

#### Application to real EEG data

The coherence matrices for the spontaneous activity data have been estimated and analyzed around the individual alpha frequency, IAF (Klimesch, 1999), of the subject (i.e. 10 Hz). In Fig. 13, the maps of the imaginary coherence and for the classical coherence (magnitude of the coherence) at the frequency corresponding to the IAF are presented. Both of the coherence measures have been derived for the average (b, f), cephalic (c, g), digitally linked mastoids (d, h) and standardized (a, e) references. From the imaginary part of the coherence, the modification of the map pattern according to the reference chosen for the data representation can be easily observed in Figs. 13(b, c, d), whereas from the coherence magnitude (f, g, h) the reference effect is secondary to the volume conduction effect, although a slight modification of the pattern attributable to the reference artifact can still be observed. Therefore, the elimination of the reference interference, in this case, would result in a minor correction with

respect to the huge effect of the volume conduction interference appearing as a strong interaction between one channel and its neighbors in (f), (g) and (h) as well as in (e) for the standardized data. The use of the imaginary part of the coherence as a measure of interaction results, on the other hand, in the elimination of self-interaction due to volume conduction. Furthermore, when data are referred to the standardized reference, a more plausible interaction pattern is obtained in comparison to other references. The pattern shown in (a), in fact, evidences an interaction between occipital and parietal electrodes that has already been reported for the same kind of data (Nunez et al., 2001).

For real data it is difficult to assess which pattern best represents the actual brain dynamics. We here argue that the REST transformed data result in the least structured maps containing smooth and simple spatial patterns. Although it is theoretically possible that a structure introduced by a reference cancels the true structure generated by the sources, we consider this as an unlikely coincidence and regard the simplest pattern as the most plausible one.

#### Comparison with different approaches

As we showed, when an analysis is done on a channel level the reference choice is fundamental. This also affects imaginary coherence in the sense that the channels are a rough estimator of the locations of interacting sources. The effect of referencing can largely be reduced by performing an inverse calculation, rather than just looking at channel level, taking the reference properly into account in the forward model. If an inverse method is able to separate all sources, it is also not necessary to restrict the analysis to the imaginary part of coherence. However, this is hardly ever

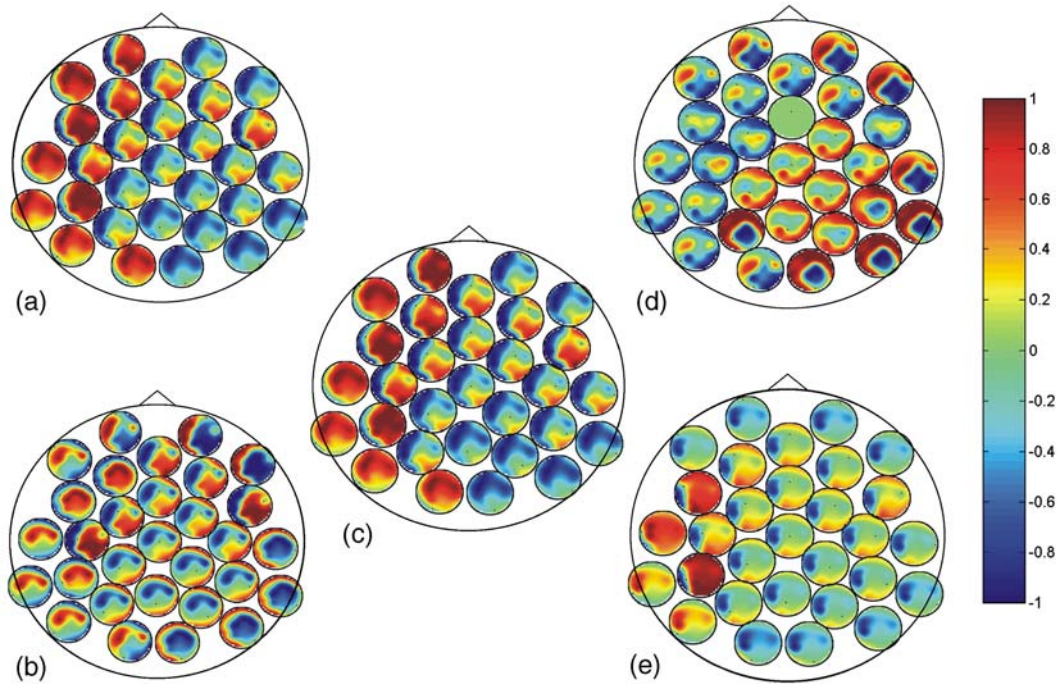


Fig. 12. Imaginary part of complex coherence (8 Hz) derived in the case of simulation 6 in which all of three sources are coherent. The map for the infinity reference case  $C_{inf}$  is shown in the middle (c); the map for the standardized data  $C_{std}$  is shown in the upper left (a), the map for the average reference data  $C_{avg}$  is shown in the lower left (b); on the right, the map for the cephalic reference data  $C_{Fcz}$  is shown in the upper right (d) and the map for the digitally linked mastoids reference  $C_{dlm}$  is shown in the lower right (e).

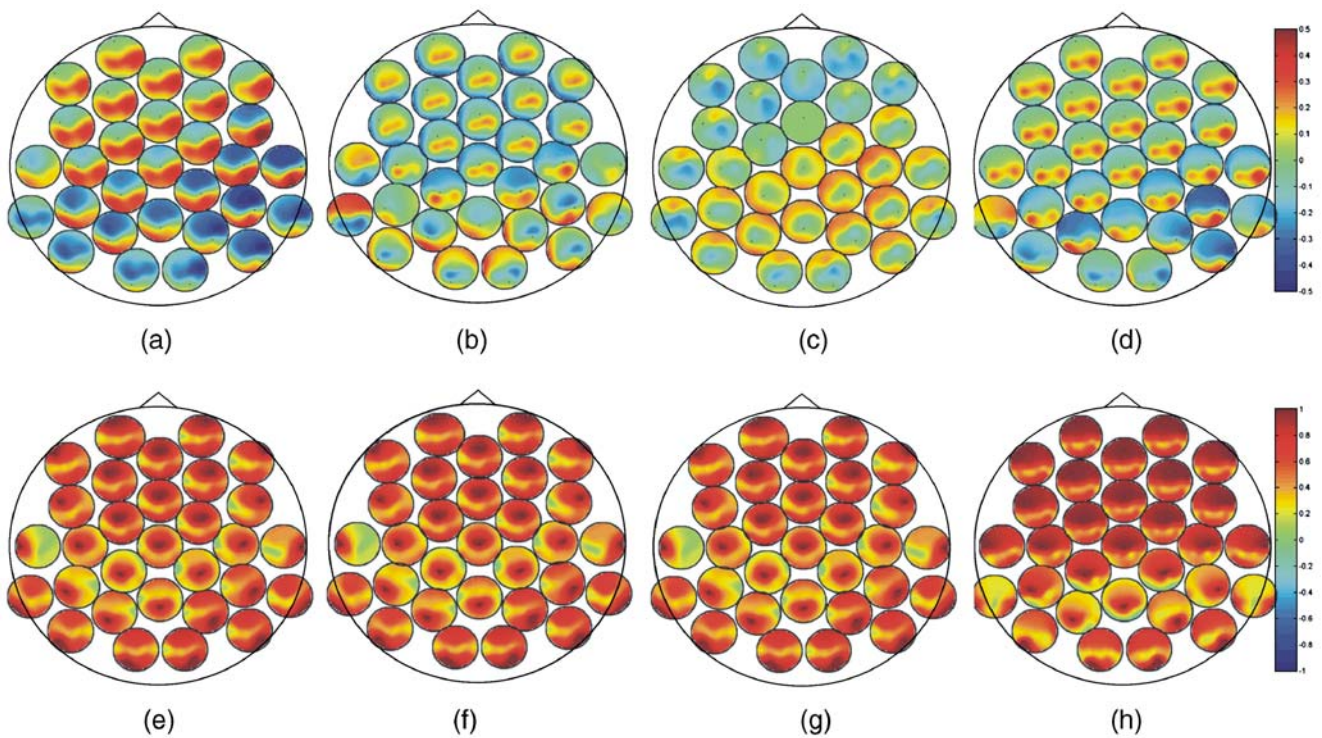


Fig. 13. In the first row the imaginary part of complex coherence estimated from human spontaneous activity data at the individual alpha frequency (10 Hz) is shown for the standardized data (a), for the average reference data (b), for the cephalic reference (c) and for the digitally linked mastoids reference (d). In the second row the module of complex coherence from the same data is shown for the standardized data (e), for the average reference data (f), for the cephalic reference (g) and for the digitally linked mastoids reference (h).

the case. It is well known that distributed source models lead to smeared source estimates for truly point-like sources. Since this smearing is a systematic effect, it is merely a question of how much averaging is needed to show significant coherence between any two brain locations even if all sources are truly independent. We therefore believe that the concept of analyzing imaginary coherency can also be of value if an analysis is performed in an estimated source space.

A mid-way between a source-level analysis and a channel-level analysis is represented by scalp techniques such as the Laplacian or the Current Source Density (CSD). These methods also address the problem of getting rid of reference effects.

The Current Source Density (CSD) approach (Nunez and Srinivasan, 2006) aims at estimating the current density on the scalp that is generated by the electrical activity of the brain; because current density is a property of points on the scalp, it is strictly reference-free. Although this approach provides an elegant solution to the reference problem in theory, it has the limitation that the CSD transformation is essentially a spatial high-pass filter that has the beneficial effect of removing potentials due to distant sources, but which also attenuates sources that are widely distributed. When the activity tends to show broad scalp distributions, a CSD transformation may eliminate the very activity that is of interest. In analogy, the nearest-neighbor Laplacian (Hjorth, 1975) and the more accurate spline-Laplacian (Perrin et al., 1987) may sometimes underestimate coherence measured as the magnitude of complex coherency as a consequence of the high pass nature of surface Laplacian (Nunez et al., 2006). Nevertheless, a quantitative evaluation of the performance of surface Laplacian as a method to get rid of the reference effect when used in combination with the imaginary part of the coherency can be investigated in the future and compared to the REST performances.

## Conclusions

In this work we investigated the study of large scale EEG coherence on simulated and measured EEG data using the imaginary part of complex coherency, a measure that is able to get rid of the artifactual self-interaction introduced in the magnitude of the complex coherency by the volume conduction effect. As a consequence, the high degree of coherence between one channel and its neighbors, which is the typical effect of volume conduction, is removed from our maps.

Due to the physical impossibility of measuring a reference-free electric potential, EEG data are usually referenced to a particular electrode. However, if there is a neural electric activity at the reference site it will contribute to the recordings of all channels. The reference choice has, therefore, substantial effects on the analysis and the interpretation of EEG data. The optimal choice of the reference site depends on the particular study and on the purpose of the analysis (Dien, 1998).

This work aims at showing the effect of the reference choice on the study of brain interactions based on complex coherency. We show that the influence of an active reference on the coherency maps can be significantly reduced by the offline transformation of the EEG data obtained with the standardization procedure. From the investigations on simulated data, we can conclude that the perturbations introduced by the physical references in the EEG, which significantly alter the interpretation of the coherency maps in terms of interactions, can be successfully eliminated by the use of coherency mapping based on standardized data.

Although the performances of the standardization depend on the actual source parameters, we have shown that for any of the proposed configurations the standardized data are a better approximation of the theoretical infinity reference potential than any of the other investigated references commonly used in coherency mapping. Furthermore, the performances of the other references (i.e. average, digitally linked mastoids, cephalic) also depend on the source parameters so that the optimal choice of the reference site depends on the particular study and on the purpose of the analysis.

The use of standardized data together with the choice of the imaginary part of complex coherency as a measure of interaction represents an appropriate, optimal choice to improve the analysis of EEG data that is able to remove the reference effect and the volume conduction artifact in the study of spectral and coherency properties of the EEG signal at the same time. Moreover, since the REST transformation is a standardized procedure, a spectral and coherency mapping based on such data facilitates the comparison of results obtained from different EEG laboratories or stored with respect to different references in databases collected over time. We propose this approach for a simultaneously unbiased and reliable comparison and integration of large scale interaction results obtained on the basis of large scale coherency EEG.

## References

- Cantero, J.L., Atienza, M., Salas, R.M., 2000. Clinical value of EEG coherence as electrophysiological index of cortico-cortical connections during sleep. *Rev. Neurol.* 31 (5), 442–454.
- Dien, J., 1998. Issues in the application of the average reference: review, critiques, and recommendations. *Behav. Res. Methods Instrum. Comput.* 30 (1), 34–43.
- Geselowitz, D.B., 1998. The zero of potential. *IEEE Eng. Med. Biol.* 17, 128–132.
- Hjorth, B., 1975. An on line transformation of EEG scalp potential into orthogonal source derivations. *Electroencephalogr. Clin. Neurophysiol.* 39, 526–530.
- Huizenga, H.M., Molenaar, P.C.M., 1996. Ordinary least squares dipole localization is influenced by the reference. *Electroencephalogr. Clin. Neurophysiol.* 99, 562–567.
- Klimesch, W., 1999. EEG alpha and theta oscillations reflect cognitive and memory performance: a review and analysis. *Brain Res. Brain Res. Rev.* 29, 169–195.
- Nolte, G., Bai, U., Wheaton, L., Mari, Z., Vorbach, S., Hallett, M., 2004. Identifying true brain interaction from EEG data using the imaginary part of coherency. *Clin. Neurophysiol.* 115, 2292–2307.
- Nunez, P.L., 2000. Toward a quantitative description of large scale neocortical dynamic function and EEG. *Behav. Brain Sci.* 23, 371–437.
- Nunez, P.L., Srinivasan, R., 2006. *Electric Fields of the Brain. The Neurophysics of EEG.* Oxford Univ. Press, New York, pp. 73–75.
- Nunez, P.L., Srinivasan, R., Westdorp, A.F., Wijesinghe, R.S., Tucker, D.M., Silberstein, R.B., Cadusch, P.J., 1997. EEG coherency I: statistics, reference electrode, volume conduction, Laplacians, cortical imaging, and interpretation at multiple scales. *Electroencephalogr. Clin. Neurophysiol.* 103, 499–515.
- Nunez, P.L., Wingeier, B.M., Silberstein, R.B., 2001. Spatial–Temporal structures of human alpha rhythms: theory, microcurrent sources, multiscale measurements, and global binding of local networks. *Hum. Brain Mapp.* 13, 125–164.
- Offner, F., 1950. The EEG as potential mapping: the value of the average monopolar reference. *Electroencephalogr. Clin. Neurophysiol.* 2, 215–216.

- Pascual-Marqui, R.D., Lehmann, D., 1993. Topographical maps, sources localization inference, and the reference electrode: comments on a paper by Desmedt et al. *Electroencephalogr. Clin. Neurophysiol.* 88, 532–533.
- Perrin, F., Bertrand, O., Pernier, J., 1987. Scalp current density mapping: value and estimation from potential data. *IEEE Trans. Biomed. Eng.* BME-34, 283–288.
- Sarvas, J., 1987. Basic mathematical and electromagnetic concepts of the biomagnetic inverse problem. *Phys. Med. Biol.* 32 (1), 11–22.
- Srinivasan, R., Nunez, P.L., Silberstein, R.B., 1998. Spatial filtering and neocortical dynamics: estimates of EEG coherence. *IEEE Trans. Biomed. Eng.* 45, 814–826.
- Yao, D., 2001. A method to standardize a reference of scalp EEG recordings to a point at infinity. *Physiol. Meas.* 22, 693–711.
- Yao, D., 2003. High-resolution EEG mapping: an equivalent charge-layer approach. *Phys. Med. Biol.* 48, 1997–2011.
- Yao, D., Wang, L., Oostenveld, R., Nielsen, K.D., Arendt-Nielsen, L., Chen, A., 2005. A comparative study of different references for EEG spectral mapping: the issue of the neutral reference and the use of the infinity reference. *Physiol. Meas.* 26, 173–184.
- Zhai, Y., Yao, D., 2004. A study on the reference electrode standardization technique for a realistic head model. *Comput. Methods Programs Biomed.* 76 (3), 229–238.